



# Synthesis and Evaluation of Coumarin-Chalcone Derivatives as $\alpha$ -Glucosidase Inhibitors

Chun-Mei Hu<sup>†</sup>, Yong-Xin Luo<sup>†</sup>, Wen-Jing Wang, Jian-Ping Li, Meng-Yue Li, Yu-Fei Zhang, Di Xiao, Li Lu, Zhuang Xiong\*, Na Feng\* and Chen Li\*

School of Biotechnology and Health Sciences, Wuyi University, Jiangmen, China

## OPEN ACCESS

### Edited by:

Xi Zheng,  
Rutgers, The State University of New  
Jersey, United States

### Reviewed by:

Chaoqun Li,  
Shaanxi Normal University, China  
Yushui Bi,  
Shandong First Medical University,  
China  
Ren Qinggang,  
Guangdong University of  
Petrochemical Technology, China

### \*Correspondence:

Zhuang Xiong  
wyuchemxz@126.com  
Na Feng  
wyuchemfn@126.com  
Chen Li  
wyuchemlc@126.com

<sup>†</sup>These authors have contributed  
equally to this work

### Specialty section:

This article was submitted to  
Organic Chemistry,  
a section of the journal  
Frontiers in Chemistry

Received: 22 April 2022

Accepted: 05 May 2022

Published: 27 June 2022

### Citation:

Hu C-M, Luo Y-X, Wang W-J, Li J-P,  
Li M-Y, Zhang Y-F, Xiao D, Lu L,  
Xiong Z, Feng N and Li C (2022)  
Synthesis and Evaluation of Coumarin-  
Chalcone Derivatives as  $\alpha$ -  
Glucosidase Inhibitors.  
Front. Chem. 10:926543.  
doi: 10.3389/fchem.2022.926543

Coumarin and chalcone, two important kinds of natural product skeletons, both exhibit  $\alpha$ -glucosidase inhibitory activity. In this work, coumarin-chalcone derivatives 3 (**a-v**) were synthesized, and their  $\alpha$ -glucosidase inhibitory activity was screened. The results showed that all synthetic derivatives ( $IC_{50}$ :  $24.09 \pm 2.36$  to  $125.26 \pm 1.18 \mu M$ ) presented better  $\alpha$ -glucosidase inhibitory activity than the parent compounds 3-acetylcoumarin ( $IC_{50}$ :  $1.5 \times 10^5 \mu M$ ) and the positive control acarbose ( $IC_{50}$ :  $259.90 \pm 1.06 \mu M$ ). Among them, compound **3t** displayed the highest  $\alpha$ -glucosidase inhibitory activity ( $IC_{50}$ :  $24.09 \pm 2.36 \mu M$ ), which was approximately 10 times stronger than that of acarbose. The kinetic assay of **3t** ( $K_I = 18.82 \mu M$ ,  $K_{IS} = 59.99 \mu M$ ) revealed that these compounds inhibited  $\alpha$ -glucosidase in a mixed-type manner. Molecular docking was used to simulate the interaction between  $\alpha$ -glucosidase and compound **3t**.

**Keywords:** coumarin, chalcone,  $\alpha$ -glucosidase, enzyme inhibitor, docking

## INTRODUCTION

Type 2 diabetes mellitus (T2DM) is a metabolic disease characterized by hyperglycemia resulting from insulin resistance and insufficient insulin secretion by pancreatic  $\beta$ -cells. One of the key reasons for the hyperglycemia is the enzymatic hydrolysis of carbohydrates.  $\alpha$ -Glucosidase (EC 3.2.1.20) plays an important role in carbohydrate digestion, in which the oligosaccharides and disaccharides from dietary carbohydrates are broken down into monosaccharides. The  $\alpha$ -glucosidase inhibitors suppress the absorption and assimilation of monosaccharides and delay the digestion of carbohydrates (Cohen and Goedert, 2004; Proença et al., 2017; Xu et al., 2019; Zhong et al., 2019). Some commercially available  $\alpha$ -glucosidase inhibitors, including miglitol, voglibose, and acarbose, have been used in the clinical treatment of T2DM, but they still show several adverse effects (Chai et al., 2015; Khursheed et al., 2019; Rocha et al., 2019). In addition,  $\alpha$ -glucosidase is closely related to hepatitis, cancer, and Pompe disease (Kasturi et al., 2018; Gulcin et al., 2019). Therefore, it is always beneficial in medicinal chemistry to develop potent  $\alpha$ -glucosidase inhibitors.

Coumarin is an important natural product skeleton with various pharmacological properties; among these, its anti-hyperglycemic activity is the focus of our research (Kontogiorgis et al., 2012; Katsori and Litina, 2014; Adib et al., 2018). Previous studies have shown that natural products containing the coumarin moiety and synthesized coumarin derivatives exhibit anti-hyperglycemic activity through the inhibition of  $\alpha$ -glucosidase (Adib et al., 2018). For instance, Wang et al. (2016) reported on a series of coumarin-thiazoles with the highest  $\alpha$ -glucosidase inhibitory activity ( $IC_{50} = 6.2 \mu M$ ). Salar et al. (2016) developed 3-thiazolyl coumarins with the most potent  $\alpha$ -glucosidase inhibitory activity ( $IC_{50} = 0.12 \mu M$ ) (Salar et al., 2016). Ibrar et al. designed coumarinyl iminothiazolidinones with the most effective inhibitory activity ( $IC_{50} = 0.09 \mu M$ ) (Ibrar et al.,

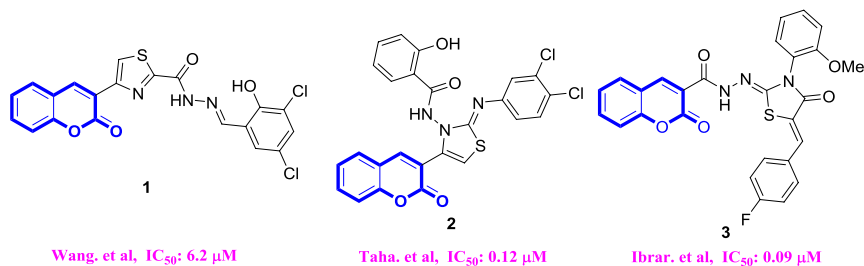
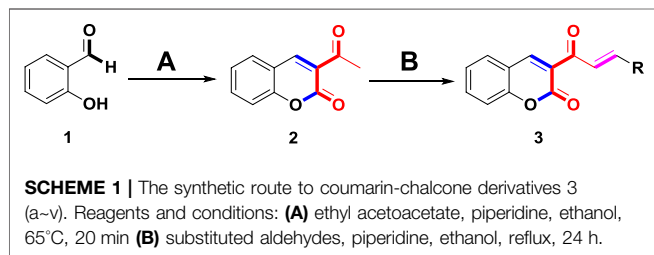


**FIGURE 1** |  $\alpha$ -glucosidase inhibitors containing coumarin.



2017). (**Figure 1**) Chalcone, an important sub-structure widely existing in many natural products, has the ability to bind to a variety of targets, resulting in many biological activities (Bak et al., 2011; Feng et al., 2014; Kang et al., 2018; Djemoui et al., 2020; Rocha et al., 2020; Dorn et al., 2010).

In medicinal chemistry, the hybrid of pharmacophore and skeleton is an effective strategy for obtaining active lead compounds. Until now, many coumarin-chalcone derivatives had been synthesized with many biological properties, such as antioxidant, anti-cancer, antibacterial, and anti-inflammatory properties (Pingaew et al., 2014; Seidel et al., 2014; Lee et al., 2018). However, there were few reports on the application of  $\alpha$ -glucosidase inhibitors. Therefore, we synthesized coumarin-chalcone derivatives **3a~v** and screened their inhibitory activity against  $\alpha$ -glucosidase.

## RESULTS AND DISCUSSION

### Chemistry

Coumarin-chalcone derivatives **3(a~v)** were prepared according to a well-known method (Roussel and Fraser, 1993; Vazquez-Rodriguez et al., 2015; Shang et al., 2018; Wang et al., 2019). In the presence of piperidine, salicylaldehyde **1** reacted with ethyl acetoacetate to produce 3-acetylcoumarin (**2**). Then 3-acetylcoumarin **2** and the substituted aldehydes underwent the aldol condensation reaction under the catalysis of piperidine to give coumarin-chalcone derivatives **3(a~v)** (**Scheme 1**). Compounds **3(a~v)** had been reported previously and the title compounds were characterized by  $^1\text{H}$  NMR.

### $\alpha$ -Glucosidase Inhibition Assay

Coumarin-chalcone derivatives **3(a~v)** were screened for their inhibitory activities against  $\alpha$ -glucosidase using 4-nitrophenyl- $\alpha$ -

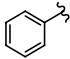
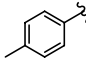
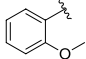
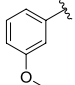
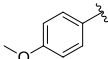
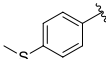
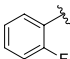
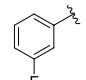
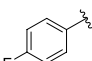
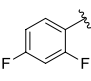
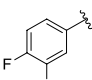
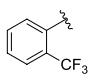
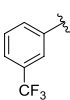
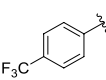
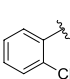
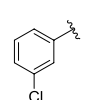
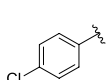
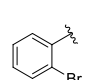
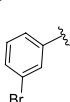
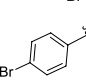
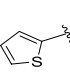
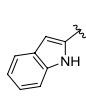
D-galactopyranoside (*p*-NPG) as a substrate and the results are summarized in **Table 1**. The parent compounds 3-acetylcoumarin only showed low inhibitory activity with  $IC_{50}$  values of  $1.5 \times 10^5$ . Interestingly, all synthetic derivatives showed moderate to good inhibitory activity towards  $\alpha$ -glucosidase with  $IC_{50}$  values ranging from  $24.09 \pm 2.36$  to  $125.26 \pm 1.18$   $\mu$ M. The results revealed that the inhibitory activities of synthetic compounds were significantly enhanced by hybridizing the two molecular skeletons. Furthermore, all the title compounds presented higher inhibitory activity than that of the positive control acarbose ( $IC_{50}$ :  $259.90 \pm 1.06$   $\mu$ M). Among them, compounds **3j**, **3q** and **3t** demonstrated the highest inhibitory activity ( $IC_{50}$ :  $30.30 \pm 2.53$ ,  $29.74 \pm 2.68$ , and  $24.09 \pm 2.36$   $\mu$ M, respectively): 10 times stronger than that of acarbose.

### Structure Activity Relationships

The structure activity relationships (SARs) of compounds **3(a~v)** was analyzed based on their  $\alpha$ -glucosidase inhibitory activities. Compound **3a** ( $IC_{50}$ :  $125.26 \pm 1.18$   $\mu$ M) without any substituent was selected as the template compound. It could be seen that the introduction of various substituents resulted in an obvious change in inhibitory activity. For compound **3b** ( $IC_{50}$ :  $95.23 \pm 1.35$   $\mu$ M) with a 4-methyl group, its inhibitory activity slightly increased compared to **3a**. For compounds **3(g~i)** with the fluorine group, **3(l~n)** with the trifluoromethyl group, **3(o~q)** with the chlorine group, and **3(r~t)** with the bromine group, all presented stronger inhibitory activity than compound **3a**, indicating that electron-withdrawing groups such as fluorine, trifluoromethyl, chlorine, and bromine could lead to an increase in inhibitory activity. Among them, **3i** with the 4-fluorine group ( $IC_{50}$ :  $35.68 \pm 0.28$   $\mu$ M), **3n** with the 4-trifluoromethyl group ( $IC_{50}$ :  $53.58 \pm 1.95$   $\mu$ M), **3q** with the 4-chlorine group ( $IC_{50}$ :  $29.74 \pm 2.68$   $\mu$ M), and **3t** with the 4-bromine group ( $IC_{50}$ :  $24.09 \pm 2.36$   $\mu$ M) showed higher inhibitory activity than the 2- and 3-position groups. For compounds **3j** and **3k** with difluoro groups, the introduction of 2,4-difluoro groups (**3j**,  $IC_{50}$ :  $30.30 \pm 2.53$ ) resulted in the stronger inhibitory activities. While for compounds **3(c~e)** with methoxy group, the 2-position group (**3c**,  $IC_{50}$ :  $60.89 \pm 2.74$ ) was better than 3-position group and 4-position group.

Furthermore, the sequencing of inhibitory activity was identified: **3t** (with 4-bromine group) > **3q** (with 4-chlorine group) > **3i** (with 4-fluorine group) > **3n** (with 4-trifluoromethyl group), predicting that stronger electron-withdrawing groups led to weaker inhibitory activity as for the compounds with electron-withdrawing groups. In addition, in the electron-withdrawing groups, inhibitory activity was

**TABLE 1** |  $\alpha$ -Glucosidase inhibitory activities of compounds **3** (a~v).

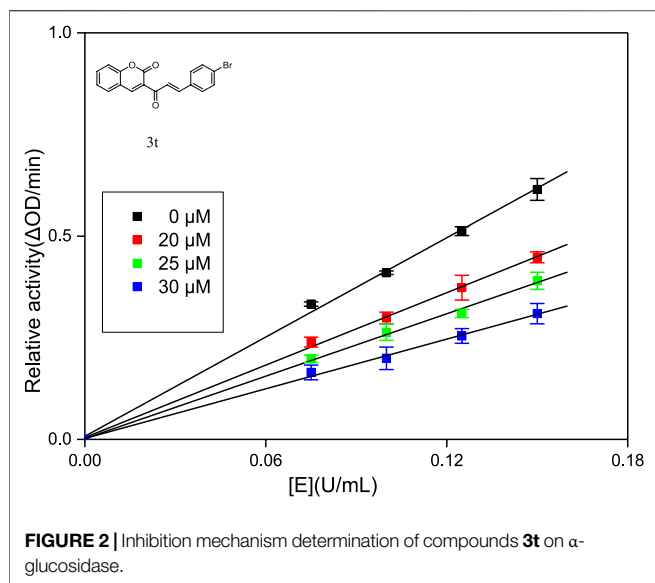
Compound	R	IC <sub>50</sub> ( $\mu$ M)	Compound	R	IC <sub>50</sub> ( $\mu$ M)
3a		125.26 $\pm$ 1.18	3b		95.23 $\pm$ 1.35
3c		60.89 $\pm$ 2.74	3d		96.39 $\pm$ 1.37
3e		105.18 $\pm$ 1.98	3f		75.53 $\pm$ 0.98
3g		48.36 $\pm$ 1.42	3h		45.68 $\pm$ 1.28
3i		35.68 $\pm$ 0.28	3j		30.30 $\pm$ 2.53
3k		49.68 $\pm$ 3.28	3l		71.52 $\pm$ 2.14
3m		64.71 $\pm$ 1.82	3n		53.58 $\pm$ 1.95
3o		59.68 $\pm$ 1.73	3p		52.62 $\pm$ 2.45
3q		29.74 $\pm$ 2.68	3r		38.56 $\pm$ 1.87
3s		35.56 $\pm$ 2.18	3t		24.09 $\pm$ 2.36
3u		109.23 $\pm$ 2.69	3v		103.31 $\pm$ 1.45
3-Acetylcoumarin		1.5 $\times$ 10 <sup>5</sup>			
Acarbose		259.90 $\pm$ 1.06			

related to the substituted position as follows: the inhibitory activity of compounds with the withdrawing groups at para-position was superior to that at meta-position, which is better than that at ortho-position. The introduction of thiophene (**3u**) or indole (**3v**) ring only slightly improved the inhibitory activity compared with compound **3a**.

### Inhibitory Mechanism Analysis

Generally, according to the type of inhibition, enzyme inhibitors can be divided into reversible inhibitors and irreversible

inhibitors (Abuelizz et al., 2019). In order to obtain the principle of the combination of enzyme inhibitors and enzymes, it is necessary to study the interaction between enzyme inhibitors and enzymes. Compounds **3j**, **3q** and **3t** with strongest inhibitory activity were chosen for the research of inhibition kinetics against  $\alpha$ -glucosidase (the inhibitory mechanism analysis of compound **3t** was shown in **Figure 2** and figures for the inhibitory mechanism analysis of compounds **3j** and **3q** have been shown in the supporting information). A series of plots of enzymatic reaction rate ( $v$ ) vs.  $\alpha$ -glucosidase



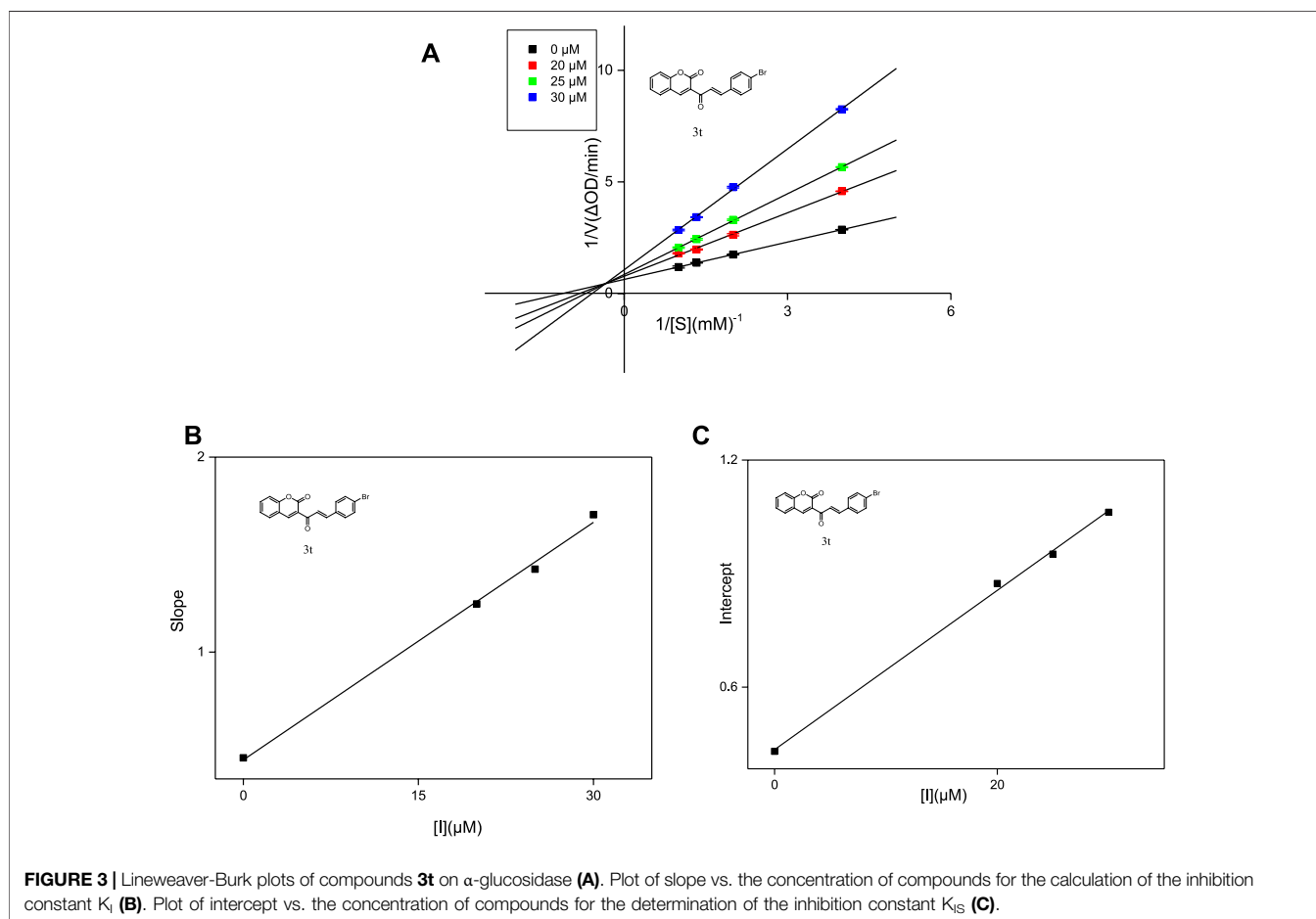
concentration in the presence of inhibitors were generated to identify the type of inhibition that is listed in **Figure 1**. The presence of **3j**, **3q** and **3t** did not change the number of enzymes

**TABLE 2** | Type of inhibition mechanism, as well as  $K_I$  and  $K_{IS}$  values of compounds **3j**, **3q** and **3t**.

Compound	Inhibition mechanism	$K_I$ ( $\mu\text{M}$ )	$K_{IS}$ ( $\mu\text{M}$ )
3j	Mixed type	19.53	25.94
3q	Mixed type	16.13	20.34
3t	Mixed type	11.02	20.71

but reduced the enzyme activity, which indicated that their inhibition mechanisms on  $\alpha$ -glucosidase were reversible.

The inhibit type of inhibitors on  $\alpha$ -glucosidase include four types, named competitive inhibition, non-competitive inhibition, mixed inhibition, and anti-competitive inhibition (Abuelizz et al., 2019). The inhibition modes of compounds **3j**, **3q** and **3t** against  $\alpha$ -glucosidase were investigated using Lineweaver-Burk double reciprocal plot. As shown in **Figure 3**, the straight lines of  $1/v$  vs.  $1/[S]$  in the presence of compounds **3j**, **3q** and **3t** intersected at a point in the second quadrant respectively, illustrating that the inhibit type of **3j**, **3q** and **3t** was mixed-type inhibition. Subsequently, the  $K_I$  values and  $K_{IS}$  values of **3j**, **3q** and **3t** were calculated based on the slope or intercept vs. PNPg concentration and summarized in **Table 2**. The higher  $K_{IS}$  values compared to  $K_I$  values indicated



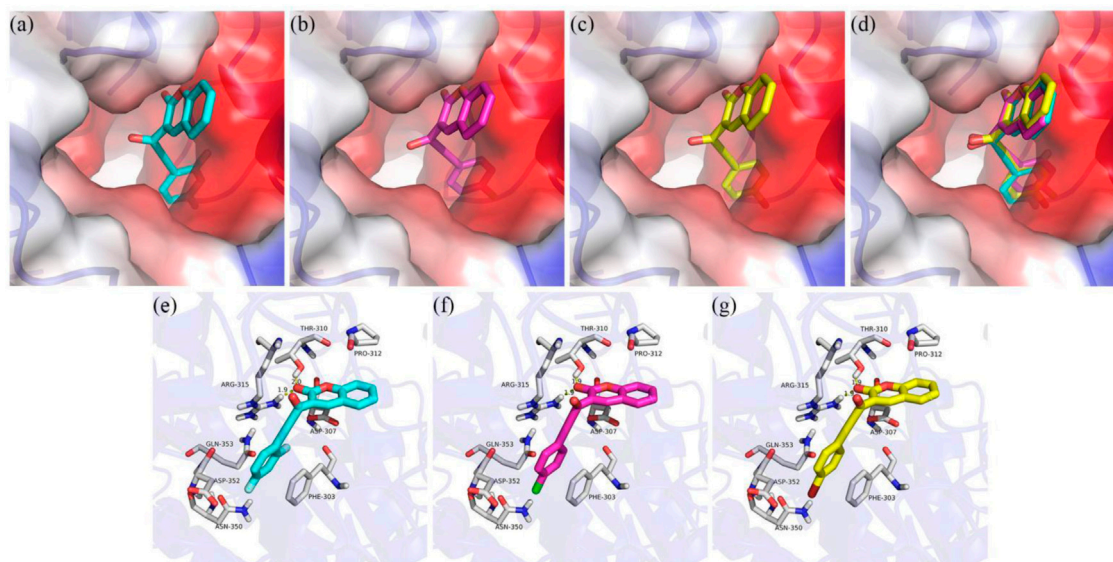


**FIGURE 4** | Molecular docking of compounds **3d**, **3f** and **3i** with  $\alpha$ -glucosidase. **(A)** Compound **3q** in the active pocket **(B)**; Compound **3t** in the active pocket **(C)**; compounds **3j**, **3q** and **3t** in the active pocket of  $\alpha$ -glucosidase **(D)**; 2D view of **3j** with  $\alpha$ -glucosidase **(E)**; 2D view of **3q** with  $\alpha$ -glucosidase **(F)**; 2D view of **3t** with  $\alpha$ -glucosidase **(G)**.

that the affinity of compounds **3j**, **3q** and **3t** with free enzyme was higher than that with enzyme-substrate complex.

### Molecular Docking Simulation

To better understand the inhibition mechanism of compounds **3j**, **3q** and **3t**, the binding modes of  $\alpha$ -glucosidase with **3j**, **3q** and **3t** were simulated using Sybyl 2.1.1 (United States) and Pymol software. The crystal structure of *Saccharomyces cerevisiae* isomaltase (PDB: 3AJ7) with 72.4% of sequence identity with  $\alpha$ -glucosidase was chosen as the target protein (Wang et al., 2017; Asgari et al., 2019; Morocho et al., 2019; Salar et al., 2016). As can be seen in **Figures 4A–D**, compounds **3j**, **3q** and **3t** had the similar interaction with the active pocket of  $\alpha$ -glucosidase. **Figures 4E–G** show that the carbonyl group of coumarin of **3j**, **3q** and **3t** all formed two hydrogen bonds with Thr310 and Arg315, respectively. Compounds **3j**, **3q** and **3t** all made a  $\pi$ - $\pi$  interaction with Phe303; and all established hydrophobic interactions with Pro310, Asp307, Asp352, Gln353, and Asn350.

### CONCLUSION

In summary, the  $\alpha$ -glucosidase inhibitory activity of coumarin-chalcone derivatives **3(a–v)** was evaluated. The results showed that all compounds presented outstanding  $\alpha$ -glucosidase inhibitory activities ( $IC_{50}$ :  $24.09 \pm 2.36$  to  $125.26 \pm 1.18 \mu\text{M}$ ) than the positive control acarbose and parent compounds 3-acetylcoumarin and benzaldehyde. Compounds **3j**, **3q**, **3t** displayed the highest  $\alpha$ -glucosidase inhibitory activity ( $IC_{50}$ :  $30.30 \pm 2.53$ ,  $29.74 \pm 2.68$ ,  $24.09 \pm$

$2.36 \mu\text{M}$ , respectively), which was approximately 10 times stronger than acarbose. Inhibition mechanism results revealed that these compounds inhibited  $\alpha$ -glucosidase in a mixed-type manner. Molecular docking verified the interactions of  $\alpha$ -glucosidase with compounds **3j**, **3q**, and **3t**.

## EXPERIMENT

### Chemicals and Instruments

Ethyl acetoacetate, salicylaldehyde and absolute ethanol were analytical pure grade and purchased from Aladdin (Shanghai) Reagent Co., Ltd. Piperidine; glacial acetic acid, petroleum ether and ethyl acetate were supplied by Titan (Shanghai) Technology Co., Ltd.;  $\alpha$ -Glucosidase from *Saccharomyces cerevisiae* (EC 3.2.1.20), 4-nitrophenyl- $\alpha$ -D-galactopyranoside (*p*-NPG), and Dimethyl sulfoxide (DMSO) were supported by Sigma-Aldrich (United States) Chemical Co., Ltd. Melting points were tested on a micro melting-point instrument.  $^1\text{H}$  NMR spectra were measured ( $\text{CDCl}_3$ ) by Bruker DPX-500 MHz AVANCE with TMS as an internal standard. Mass spectroscopy was performed on a (LCQTM). The absorbance was recorded by a micro-plate reader.

### Synthesis of 3-Acetylcoumarin

To a solution of Salicylaldehyde **1** (1.0 mmol) in ethanol (10 ml), ethyl acetoacetate (1.0 mmol) and piperidine (1.0 mmol) were added and the mixture was stirred at  $65^\circ\text{C}$  for 20 min. When the reaction was judged to be complete by TLC, the crude product was obtained by filtration, followed by washing with petroleum ether to produce 3-acetylcoumarin **2**.

Yellow solid; yield 72.3%;  $^1\text{H}$  NMR (500 MHz, Chloroform-*d*)  $\delta$  8.54 (s,  $^1\text{H}$ ), 7.70–7.66 (m, 2H), 7.42–7.36 (m, 2H) 2.76 (s, 3H).

## Synthesis of Coumarin-Chalcone Derivatives 3(a~v)

To a solution of 3-acetylcoumarin **2** (1.0 mmol) in ethanol (10 ml) substituted aromatic aldehydes (1.0 mmol) and piperidine (1.0 mmol) were added, and then the mixture was refluxed for 24 h. The crude product was obtained by filtration, and subsequently by recrystallization by ethanol to give the title compounds **3(a~v)**.

**(E)-3-[3-(cinnamoyl)-2H-chromen-2-one (3a)**. Yellow solid; yield 51.7%;  $^1\text{H}$  NMR (500 MHz, Chloroform-*d*)  $\delta$  8.60 (s,  $^1\text{H}$ ), 7.92 (dd,  $J = 40, 20$  Hz, 2H), 7.71–7.65 (m, 4H), 7.44–7.39 (m, 4H), 7.35 (t,  $J = 8, 7.5$  Hz,  $^1\text{H}$ ).

**(E)-3-[3-(*p*-tolyl) acryloyl]-2H-chromen-2-one (3b)**. Yellow solid; yield 45.9%;  $^1\text{H}$  NMR (500 MHz, Chloroform-*d*)  $\delta$  8.58 (s,  $^1\text{H}$ ), 7.84 (dd,  $J = 20, 15$  Hz, 2H), 7.69–7.62 (m, 4H), 7.39 (d,  $J = 5$  Hz,  $^1\text{H}$ ), 7.35 (td,  $J = 7.5, 1$  Hz,  $^1\text{H}$ ), 6.93 (dt,  $J = 10, 3$  Hz, 2H), 3.85 (s, 3H).

**(E)-3-[3-(2-methoxyphenyl) acryloyl]-2H-chromen-2-one (3c)**. Yellow solid; yield 37.7%;  $^1\text{H}$  NMR (500 MHz, Chloroform-*d*)  $\delta$  8.56 (s,  $^1\text{H}$ ), 8.22 (d,  $J = 15$  Hz,  $^1\text{H}$ ), 7.98 (d,  $J = 15$  Hz,  $^1\text{H}$ ), 7.73–7.62 (m, 3H), 7.42–7.32 (m, 3H), 6.99 (t,  $J = 10, 10$  Hz,  $^1\text{H}$ ), 6.93 (d,  $J = 10$  Hz,  $^1\text{H}$ ), 3.92 (s, 3H).

**(E)-3-[3-(3-methoxyphenyl) acryloyl]-2H-chromen-2-one (3d)**. yellow solid; yield 42.1%;  $^1\text{H}$  NMR (500 MHz, Chloroform-*d*)  $\delta$  8.59 (s,  $^1\text{H}$ ), 7.93 (d,  $J = 20$  Hz,  $^1\text{H}$ ), 7.71–7.65 (m, 2H), 7.41 (d,  $J = 5$  Hz,  $^1\text{H}$ ), 7.39–7.31 (m, 2H), 7.28 (d,  $J = 10$  Hz,  $^1\text{H}$ ), 7.19 (t,  $J = 5, 2$  Hz,  $^1\text{H}$ ), 6.97 (ddd,  $J = 8, 2.5, 1$  Hz,  $^1\text{H}$ ), 3.86 (s, 3H).

**(E)-3-[3-(4-methoxyphenyl) acryloyl]-2H-chromen-2-one (3e)**. Yellow solid; Yield 49.7%;  $^1\text{H}$  NMR (500 MHz, Chloroform-*d*)  $\delta$  8.58 (s,  $^1\text{H}$ ), 7.88 (dd,  $J = 30, 15$  Hz, 2H), 7.69–7.64 (m, 2H), 7.58 (d,  $J = 10$  Hz, 2H), 7.40 (d,  $J = 10$  Hz,  $^1\text{H}$ ), 7.35 (t,  $J = 10, 5$  Hz,  $^1\text{H}$ ), 7.22 (d,  $J = 10$  Hz, 2H), 2.39 (s, 3H).

**(E)-3-[3-[4-(methylthio)phenyl] acryloyl]-2H-chromen-2-one (3f)**. Yellow solid; yield 55.2%;  $^1\text{H}$  NMR (500 MHz, Chloroform-*d*)  $\delta$  8.59 (s,  $^1\text{H}$ ), 7.87 (dd,  $J = 40, 20$  Hz, 2H), 7.70–7.64 (m, 2H), 7.61–7.57 (m, 2H), 7.40 (d,  $J = 10$  Hz,  $^1\text{H}$ ), 7.35 (td,  $J = 10, 1.5$  Hz,  $^1\text{H}$ ), 7.24 (d,  $J = 10$  Hz, 2H), 2.52 (s, 3H).

**(E)-3-[3-(2-fluorophenyl) acryloyl]-2H-chromen-2-one (3g)**. Yellow solid; yield 45.0%;  $^1\text{H}$  NMR (500 MHz, Chloroform-*d*)  $\delta$  8.60 (s,  $^1\text{H}$ ), 8.01 (dd,  $J = 30, 15$  Hz, 2H), 7.74 (t,  $J = 10, 10$  Hz,  $^1\text{H}$ ), 7.71–7.65 (m, 2H), 7.42–7.34 (m, 3H), 7.19 (t,  $J = 10, 10$  Hz,  $^1\text{H}$ ), 7.12 (t,  $J = 10, 10$  Hz,  $^1\text{H}$ ).

**(E)-3-[3-(3-fluorophenyl) acryloyl]-2H-chromen-2-one (3h)**. Yellow solid; yield 35.3%;  $^1\text{H}$  NMR (500 MHz, Chloroform-*d*)  $\delta$  8.61 (s,  $^1\text{H}$ ), 7.95 (d,  $J = 20$  Hz,  $^1\text{H}$ ), 7.81 (d,  $J = 15$  Hz,  $^1\text{H}$ ), 7.71–7.66 (m, 2H), 7.45–7.36 (m, 5H), 7.19 (tdd,  $J = 8.2, 2.6, 1$  Hz,  $^1\text{H}$ ).

**(E)-3-[3-(4-fluorophenyl) acryloyl]-2H-chromen-2-one (3i)**. Yellow solid; yield 44.9%;  $^1\text{H}$  NMR (500 MHz, Chloroform-*d*)  $\delta$  8.61 (s,  $^1\text{H}$ ), 7.90 (d,  $J = 20$  Hz,  $^1\text{H}$ ), 7.84 (d,  $J = 20$  Hz,  $^1\text{H}$ ),

7.71–7.65 (m, 4H), 7.41 (d,  $J = 10$  Hz,  $^1\text{H}$ ), 7.37 (td,  $J = 8.1, 0.4$  Hz,  $^1\text{H}$ ), 7.14–7.08 (m, 2H).

**(E)-3-[3-(2,4-difluorophenyl) acryloyl]-2H-chromen-2-one (3j)**. Yellow solid; yield 44.7%;  $^1\text{H}$  NMR (500 MHz, Chloroform-*d*)  $\delta$  8.61 (s,  $^1\text{H}$ ), 7.96 (d,  $J = 15$  Hz, 2H), 7.78–7.71 (m,  $^1\text{H}$ ), 7.71–7.65 (m, 2H), 7.41 (d,  $J = 10$  Hz,  $^1\text{H}$ ), 7.39–7.35 (m,  $^1\text{H}$ ), 6.98–6.92 (m,  $^1\text{H}$ ), 6.91–6.84 (m,  $^1\text{H}$ ).

**(E)-3-[3-(3,4-difluorophenyl) acryloyl]-2H-chromen-2-one (3k)**. Yellow solid; yield 37.3%;  $^1\text{H}$  NMR (500 MHz, Chloroform-*d*)  $\delta$  8.64 (s,  $^1\text{H}$ ), 7.91 (d,  $J = 15$  Hz,  $^1\text{H}$ ), 7.78 (d,  $J = 15$  Hz,  $^1\text{H}$ ), 7.70 (dd,  $J = 10, 5$  Hz,  $^1\text{H}$ ), 7.56–7.50 (m,  $^1\text{H}$ ), 7.45–7.38 (m, 4H), 7.23 (dt,  $J = 10, 10$  Hz,  $^1\text{H}$ ).

**(E)-3-[3-[2-(trifluoromethyl) phenyl]acryloyl]-2H-chromen-2-one (3l)**. Yellow solid; yield 39.8%;  $^1\text{H}$  NMR (500 MHz, Chloroform-*d*)  $\delta$  8.63 (s,  $^1\text{H}$ ), 7.94 (dd,  $J = 10, 5$  Hz, 2H), 7.74–7.58 (m, 4H), 7.53–7.48 (m,  $^1\text{H}$ ), 7.45–7.34 (m, 3H).

**(E)-3-[3-[3-(trifluoromethyl) phenyl]acryloyl]-2H-chromen-2-one (3m)**. Yellow solid; yield 39.9%;  $^1\text{H}$  NMR (500 MHz, Chloroform-*d*)  $\delta$  8.62 (s,  $^1\text{H}$ ), 7.86 (dd,  $J = 10, 5$  Hz, 3H), 7.71–7.65 (m, 3H), 7.57–7.53 (m,  $^1\text{H}$ ), 7.44–7.34 (m, 3H).

**(E)-3-[3-[4-(trifluoromethyl) phenyl]acryloyl]-2H-chromen-2-one (3n)**. Yellow solid; yield 41.4%;  $^1\text{H}$  NMR (500 MHz, Chloroform-*d*)  $\delta$  8.63 (s,  $^1\text{H}$ ), 7.86 (d,  $J = 15$  Hz,  $^1\text{H}$ ), 7.78 (d,  $J = 10$  Hz, 2H), 7.72–7.65 (m, 3H), 7.44–7.36 (m, 3H).

**(E)-3-[3-(2-chlorophenyl) acryloyl]-2H-chromen-2-one (3o)**. Yellow solid; yield 51.2%;  $^1\text{H}$  NMR (500 MHz, Chloroform-*d*)  $\delta$  8.61 (s,  $^1\text{H}$ ), 8.03 (d,  $J = 15$  Hz,  $^1\text{H}$ ), 7.79 (d,  $J = 15$  Hz,  $^1\text{H}$ ), 7.70–7.66 (m, 3H), 7.58 (d,  $J = 10$  Hz,  $^1\text{H}$ ), 7.46–7.35 (m, 4H).

**(E)-3-[3-(3-chlorophenyl) acryloyl]-2H-chromen-2-one (3p)**. Yellow solid; yield 36.4%;  $^1\text{H}$  NMR (500 MHz, Chloroform-*d*)  $\delta$  8.61 (s,  $^1\text{H}$ ), 7.95 (d,  $J = 15$  Hz,  $^1\text{H}$ ), 7.78 (d,  $J = 15$  Hz,  $^1\text{H}$ ), 7.71–7.64 (m, 3H), 7.55 (d,  $J = 10$  Hz,  $^1\text{H}$ ), 7.43–7.34 (m, 4H).

**(E)-3-[3-(4-chlorophenyl)acryloyl]-2H-chromen-2-one (3q)**. Yellow solid; yield 45.2%;  $^1\text{H}$  NMR (500 MHz, Chloroform-*d*)  $\delta$  8.61 (s,  $^1\text{H}$ ), 7.93 (d,  $J = 15$  Hz,  $^1\text{H}$ ), 7.81 (d,  $J = 15$  Hz,  $^1\text{H}$ ), 7.70–7.65 (m, 2H), 7.63 (dt,  $J = 8.5, 2.5$  Hz, 2H), 7.42–7.34 (m, 4H).

**(E)-3-[3-(2-bromophenyl)acryloyl]-2H-chromen-2-one (3r)**. Yellow solid; yield 40.8%;  $^1\text{H}$  NMR (500 MHz, Chloroform-*d*)  $\delta$  8.62 (s,  $^1\text{H}$ ), 8.24 (d,  $J = 15$  Hz,  $^1\text{H}$ ), 7.90 (d,  $J = 15$  Hz,  $^1\text{H}$ ), 7.83 (dd,  $J = 10, 5$  Hz,  $^1\text{H}$ ), 7.72–7.66 (m, 2H), 7.63 (dd,  $J = 10, 5$  Hz,  $^1\text{H}$ ), 7.41 (d,  $J = 10$  Hz,  $^1\text{H}$ ), 7.39–7.34 (m, 2H), 7.28–7.22 (m,  $^1\text{H}$ ).

**(E)-3-[3-(3-bromophenyl)acryloyl]-2H-chromen-2-one (3s)**. Yellow solid; yield 41.8%;  $^1\text{H}$  NMR (500 MHz, Chloroform-*d*)  $\delta$  8.61 (s,  $^1\text{H}$ ), 7.94 (d,  $J = 15$  Hz,  $^1\text{H}$ ), 7.82–7.75 (m, 2H), 7.70–7.65 (m, 2H), 7.59 (d,  $J = 10$  Hz,  $^1\text{H}$ ), 7.53 (ddd,  $J = 3, 1.5, 1$  Hz,  $^1\text{H}$ ), 7.43–7.35 (m, 2H), 7.29 (t,  $J = 10, 10$  Hz,  $^1\text{H}$ ).

**(E)-3-[3-(4-bromophenyl)acryloyl]-2H-chromen-2-one (3t)**. Yellow solid; yield 44.5%;  $^1\text{H}$  NMR (500 MHz, Chloroform-*d*)  $\delta$  8.61 (s,  $^1\text{H}$ ), 7.95 (d,  $J = 15$  Hz,  $^1\text{H}$ ), 7.79 (d,  $J = 15$  Hz,  $^1\text{H}$ ), 7.70–7.65 (m, 2H), 7.54 (s, 4H), 7.41 (d,  $J = 10$  Hz,  $^1\text{H}$ ), 7.36 (td,  $J = 5, 1$  Hz,  $^1\text{H}$ ).

**(E)-3-[3-(thiophen-2-yl)acryloyl]-2H-chromen-2-one (3u).** Yellow solid; yield 40.7%;  $^1\text{H}$  NMR (500 MHz,  $\text{DMSO}-d_6$ )  $\delta$  12.00 (s,  $^1\text{H}$ ), 8.68 (s,  $^1\text{H}$ ), 8.01 (d,  $J = 15$  Hz,  $^1\text{H}$ ), 8.10–8.04 (m, 2H), 7.98 (td,  $J = 10, 3.5$  Hz, 2H), 7.78–7.73 (m,  $^1\text{H}$ ), 7.69 (d,  $J = 15$  Hz,  $^1\text{H}$ ), 7.54–7.49 (m, 2H), 7.44 (td,  $J = 10, 1.5$  Hz,  $^1\text{H}$ ), 7.30–7.22 (m, 2H).

**(E)-3-[3-( $^1\text{H}$ -indol-2-yl)acryloyl]-2H-chromen-2-one (3v).** Yellow solid; yield 51.7%;  $^1\text{H}$  NMR (500 MHz, Chloroform- $d$ )  $\delta$  8.60 (s,  $^1\text{H}$ ), 7.92 (dd,  $J = 40, 20$  Hz, 2H), 7.71–7.65 (m, 4H), 7.44–7.39 (m, 4H), 7.35 (t,  $J = 8, 7.5$  Hz,  $^1\text{H}$ ).

## $\alpha$ -Glucosidase Inhibition and Kinetics Mechanism Analysis Assay

The  $\alpha$ -glucosidase inhibitory activity assay of coumarin-chalcone derivatives 3 (a–v) was conducted using *p*-NPG as a substrate. (Pogaku et al., 2019; Saeedi et al., 2019; Xu et al., 2019). 10  $\mu\text{l}$  of the test compound and 10  $\mu\text{l}$  of the enzyme (final concentration 0.1 U/ml) were added to 130  $\mu\text{l}$  of PBS (0.1 M phosphate, pH 6.8), and incubated at 37°C for 10 min. Then *p*-NPG (final concentration 0.25 mM) was added and the absorbance change was measured by a micro-plate reader at 405 nm. All experiments were assayed four times. The percentage of inhibition was obtained using the formula: Inhibition (%) =  $[(\text{OD}_1 - \text{OD}_0)/\text{OD}_0] \times 100\%$ , where  $\text{OD}_1$  and  $\text{OD}_0$  represent the absorbance value of the experimental group and the blank group respectively. Acarbose as a positive sample was also tested. The  $\text{IC}_{50}$  value of each compound was obtained from the fitting curve of inhibition vs. compound concentration.

The type of inhibition was identified by the plots of enzymatic reaction rate ( $V$ ) vs.  $\alpha$ -glucosidase concentration. The test method was similar to the above enzyme activity assay. In the presence of different concentrations of compounds 3j, 3q and 3t, respectively (0, 25, 30, and 40  $\mu\text{M}$ ), the absorbance change was detected under different concentrations of  $\alpha$ -glucosidase (0.075, 0.1, 0.125, and 0.15 U/mL).

The inhibition mode was also detected using a similar method to that described above. In the presence of different concentrations of compounds 3j, 3q and 3t, respectively (0, 25, 30 and 40  $\mu\text{M}$ ), the absorbance change was measured under different concentrations of *p*-NPG (0.25, 0.5, 0.75, 1 mM). The inhibition mode of the inhibitor was obtained using Lineweaver–Burk plots. The constant  $K_1$  was obtained by secondary plots of the derivatives concentration (I) vs. Slope, constant  $K_{1S}$  was obtained by secondary plots of the derivatives concentration (I) vs. Intercept.

## Molecular Docking

The molecular docking of  $\alpha$ -glucosidase with compounds 3d, 3f, and 3i was simulated with Sybyl 2.1.1 (United States) and Pymol software. First, compounds 3d, 3f, and 3i were prepared by energy minimization with the Tripos force field by the Powell gradient algorithm with Gasteiger–Hückel charges. The

maximum iterations for the minimization were set to 10 000. The minimization was terminated when an energy gradient convergence criterion of 0.005 kcal mol $^{-1}$  Å $^{-1}$  was reached. The energy convergence criterion of 0.01 kcal/mol and the maximum iterations for the minimization of 1,000 times were reached. Next, the crystal structure of *Saccharomyces cerevisiae* isomaltase (PDB: 3AJ7) was downloaded from the RCSB Protein Data Bank. The protein was prepared by biopolymer and implemented following the procedure of removing water molecules, adding hydrogen atoms, and repairing end residues. The active pocket of protein was generated with the automatic mode. Then the molecular docking of protein with 3d, 3f, and 3i was operated in the default format. The Pymol software was used to draw the view of protein with 3d, 3f, and 3i.

## DATA AVAILABILITY STATEMENT

The original contributions presented in the study are included in the article/Supplementary Material, further inquiries can be directed to the corresponding authors.

## AUTHOR CONTRIBUTIONS

C-MH, Y-XL, W-JW, J-PL, and M-YL dedicated to the synthesis of compounds; C-MH, Y-XL, Y-FZ, DX, and LL dedicated to the characterization of compounds and analysis of data. C-MH, Y-XL, W-JW, J-PL, and LL dedicated to the enzyme inhibition assay and enzyme kinetics assay; C-MH and Y-XL carried out the molecular docking simulation. ZX and NF designed and managed the experiments. CL supervised the work and prepared the manuscript.

## FUNDING

This work was financially supported by the Fundamental and Applied Basic Research Fund of Guangdong Province (No. 2022A1515011657), Department of Education of Guangdong Province (Nos. 2019KZDXM035, 2021KTSCX135, 2021KCXTD044), and Jiangmen Science and Technology Plan Project (2021030103150006664).

## SUPPLEMENTARY MATERIAL

The Supplementary Material for this article can be found online at: <https://www.frontiersin.org/articles/10.3389/fchem.2022.926543/full#supplementary-material>

## REFERENCE

Abuelizz, H. A., Anouar, E. H., Ahmad, R., Azman, N. I. I. N., Marzouk, M., and Al-Salahi, R. (2019). Triazolozinazoles as a New Class of Potent  $\alpha$ -glucosidase

Inhibitors: *In Vitro* Evaluation and Docking Study. *PLoS One* 14, e0220379. doi:10.1371/journal.pone.0220379  
Adib, M., Peytam, F., Rahmanian-Jazi, M., Mohammadi-Khanapostani, M., Mahernia, S., Bijanzadeh, H. R., et al. (2018). Design, Synthesis and *In Vitro*  $\alpha$ -glucosidase Inhibition of Novel Coumarin-Pyridines as Potent

- Antidiabetic Agents. *New J. Chem.* 42, 17268–17278. doi:10.1039/C8NJ02495B
- Asgari, M. S., Mohammadi-Khanaposhtani, M., Kiani, M., Ranjbar, P. R., Zabihi, E., Pourbagher, R., et al. (2019). Biscoumarin-1,2,3-triazole Hybrids as Novel Antidiabetic Agents: Design, Synthesis, *In Vitro*  $\alpha$ -glucosidase Inhibition, Kinetic, and Docking Studies. *Bioorg. Chem.* 92, 103206. doi:10.1016/j.bioorg.2019.103206
- Bak, E.-J., Park, H.-G., Lee, C.-H., Lee, T.-I., Woo, G.-H., Na, Y.-H., et al. (2011). Effects of Novel Chalcone Derivatives on  $\alpha$ -glucosidase, Dipeptidyl Peptidase-4, and Adipocyte Differentiation *In Vitro*. *BMB Rep.* 44, 410–414. doi:10.5483/BMBRep.2011.44.6.410
- Chai, T.-T., Kwek, M.-T., Ong, H.-C., and Wong, F.-C. (2015). Water Fraction of Edible Medicinal Fern *Stenochlaena palustris* Is a Potent  $\alpha$ -glucosidase Inhibitor with Concurrent Antioxidant Activity. *Food Chem.* 186, 26–31. doi:10.1016/j.foodchem.2014.12.099
- Cohen, P., and Goedert, M. (2004). GSK3 Inhibitors: Development and Therapeutic Potential. *Nat. Rev. Drug Discov.* 3, 479–487. doi:10.1038/nrd1415
- Djemoui, A., Naouri, A., Ouahrani, M. R., Djemoui, D., Lahcene, S., Lahrech, M. B., et al. (2020). A Step-by-step Synthesis of Triazole-Benzimidazole-Chalcone Hybrids: Anticancer Activity in Human Cells. *J. Mol. Struct.* 1204, 127487. doi:10.1016/j.molstruc.2019.127487
- Dorn, C., Kraus, B., Motyl, M., Weiss, T. S., Gehrig, M., Schölmerich, J., et al. (2010). Xanthohumol, a Chalcone Derived from Hops, Inhibits Hepatic Inflammation and Fibrosis. *Mol. Nutr. Food Res.* 54 (Suppl. 2), S205–S213. doi:10.1002/mnfr.200900314
- Feng, L., Maddox, M. M., Alam, M. Z., Tsutsumi, L. S., Narula, G., Bruhn, D. F., et al. (2014). Synthesis, Structure-Activity Relationship Studies, and Antibacterial Evaluation of 4-Chromanones and Chalcones, as Well as Olympicin A and Derivatives. *J. Med. Chem.* 57, 8398–8420. doi:10.1021/jm500853v
- Gulcin, I., Kaya, R., Goren, A. C., Akincioglu, H., Topal, M., Bingol, Z., et al. (2019). Anticholinergic, Antidiabetic and Antioxidant Activities of Cinnamon (Cinnamomum Verum) Bark Extracts: Polyphenol Contents Analysis by LC-MS/MS. *Int. J. Food Prop.* 22, 1511–1526. doi:10.1080/10942912.2019.1656232
- Ibrar, A., Zaib, S., Khan, I., Shafique, Z., Saeed, A., and Iqbal, J. (2017). New Prospects for the Development of Selective Inhibitors of  $\alpha$ -glucosidase Based on Coumarin-Iminothiazolidinone Hybrids: Synthesis, *In-Vitro* Biological Screening and Molecular Docking Analysis. *J. Taiwan Inst. Chem. Eng.* 81, 119–133. doi:10.1016/j.jtice.2017.09.041
- Kang, L., Gao, X.-H., Liu, H.-R., Men, X., Wu, H.-N., Cui, P.-W., et al. (2018). Structure-activity Relationship Investigation of Coumarin-Chalcone Hybrids with Diverse Side-Chains as Acetylcholinesterase and Butyrylcholinesterase Inhibitors. *Mol. Divers.* 22, 893–906. doi:10.1007/s11030-018-9839-y
- Kasturi, S. P., Surarapu, S., Uppalanchi, S., Dwivedi, S., Yogeewari, P., Sigalappali, D. K., et al. (2018). Synthesis, Molecular Modeling and Evaluation of  $\alpha$ -glucosidase Inhibition Activity of 3,4-dihydroxy Piperidines. *Eur. J. Med. Chem.* 150, 39–52. doi:10.1016/j.ejmech.2018.02.072
- Katsori, A.-M., and Hadjipavlou-Litina, D. (2014). Coumarin Derivatives: an Updated Patent Review (2012 - 2014). *Expert Opin. Ther. Pat.* 24, 1323–1347. doi:10.1517/13543776.2014.972368
- Khursheed, R., Singh, S. K., Wadhwa, S., Kapoor, B., Gulati, M., Kumar, R., et al. (2019). Treatment Strategies against Diabetes: Success So Far and Challenges Ahead. *Eur. J. Pharmacol.* 862, 172625. doi:10.1016/j.ejphar.2019.172625
- Kontogiorgis, C., Detsi, A., and Hadjipavlou-Litina, D. (2012). Coumarin-based Drugs: a Patent Review (2008 - Present). *Expert Opin. Ther. Pat.* 22, 437–454. doi:10.1517/13543776.2012.678835
- Lee, S. Y., Chiu, Y. J., Yang, S. M., Chen, C. M., Huang, C. C., Lee-Chen, G. J., et al. (2018). Novel Synthetic Chalcone-coumarin Hybrid for A $\beta$  Aggregation Reduction, Antioxidation, and Neuroprotection. *CNS Neurosci. Ther.* 24, 1286–1298. doi:10.1111/cns.13058
- Morocho, V., Sarango, D., Cruz-Erazo, C., Cumbicus, N., Cartuche, L., and Suárez, A. I. (2019). Chemical Constituents of Croton Thurifer Kunth as  $\alpha$ -Glucosidase Inhibitors. *Rec. Nat. Prod.* 14, 31–41. doi:10.25135/rnp.136.18.11.1069
- Pingaew, R., Saekee, A., Mandi, P., Nantasenammat, C., Prachayasittikul, S., Ruchirawat, S., et al. (2014). Synthesis, Biological Evaluation and Molecular Docking of Novel Chalcone-Coumarin Hybrids as Anticancer and Antimalarial Agents. *Eur. J. Med. Chem.* 85, 65–76. doi:10.1016/j.ejmech.2014.07.087
- Pogaku, V., Gangarapu, K., Basavojju, S., Tatapudi, K. K., and Katragadda, S. B. (2019). Design, Synthesis, Molecular Modelling, ADME Prediction and Anti-hyperglycemic Evaluation of New Pyrazole-Triazolopyrimidine Hybrids as Potent  $\alpha$ -glucosidase Inhibitors. *Bioorg. Chem.* 93, 103307. doi:10.1016/j.bioorg.2019.103307
- Proença, C., Freitas, M., Ribeiro, D., Oliveira, E. F. T., Sousa, J. L. C., Tomé, S. M., et al. (2017).  $\alpha$ -Glucosidase Inhibition by Flavonoids: an *In Vitro* and *In Silico* Structure-Activity Relationship Study. *J. Enzyme Inhibition Med. Chem.* 32, 1216–1228. doi:10.1080/14756366.2017.1368503
- Rocha, S., Ribeiro, D., Fernandes, E., and Freitas, M. (2020). A Systematic Review on Anti-diabetic Properties of Chalcones. *Curr. Med. Chem.* 27, 2257–2321. doi:10.2174/092986732566618100112226
- Rocha, S., Sousa, A., Ribeiro, D., Correia, C. M., Silva, V. L. M., Santos, C. M. M., et al. (2019). A Study towards Drug Discovery for the Management of Type 2 Diabetes Mellitus through Inhibition of the Carbohydrate-Hydrolyzing Enzymes  $\alpha$ -amylase and  $\alpha$ -glucosidase by Chalcone Derivatives. *Food Funct.* 10, 5510–5520. doi:10.1039/C9FO01298B
- Roussel, M. R., and Fraser, S. J. (1993). Global Analysis of Enzyme Inhibition Kinetics. *J. Phys. Chem.* 97, 8316–8327. doi:10.1021/j100133a031
- Saeedi, M., Mohammadi-Khanaposhtani, M., Asgari, M. S., Eghbalnejad, N., Imanparast, S., Faramarzi, M. A., et al. (2019). Design, Synthesis, *In Vitro* and *In Silico* Studies of Novel Diarylimidazole-1,2,3-Triazole Hybrids as Potent  $\alpha$ -glucosidase Inhibitors. *Bioorg. Med. Chem.* 27, 115148. doi:10.1016/j.bmc.2019.115148
- Salar, U., Taha, M., Khan, K. M., Ismail, N. H., Imran, S., Perveen, S., et al. (2016). Syntheses of New 3-thiazolyl Coumarin Derivatives, *In Vitro*  $\alpha$ -glucosidase Inhibitory Activity, and Molecular Modeling Studies. *Eur. J. Med. Chem.* 122, 196–204. doi:10.1016/j.ejmech.2016.06.037
- Seidel, C., Schneckeburger, M., Zwergel, C., Gaascht, F., Mai, A., Dicato, M., et al. (2014). Novel Inhibitors of Human Histone Deacetylases: Design, Synthesis and Bioactivity of 3-alkenylcoumarins. *Bioorg. Med. Chem. Lett.* 24, 3797–3801. doi:10.1016/j.bmcl.2014.06.067
- Shang, Y.-j., Wei, Q., and Sun, Z.-b. (2018). Studying the Cytotoxicity of Coumarin-Chalcone Hybrids by a Prooxidant Strategy in A549 Cells. *Monatsh Chem.* 149, 2287–2292. doi:10.1007/s00706-018-2273-0
- Vazquez-Rodriguez, S., Lama López, R., Matos, M. J., Armesto-Quintas, G., Serra, S., Uriarte, E., et al. (2015). Design, Synthesis and Antibacterial Study of New Potent and Selective Coumarin-Chalcone Derivatives for the Treatment of Tenacibaculosis. *Bioorg. Med. Chem.* 23, 7045–7052. doi:10.1016/j.bmc.2015.09.028
- Wang, G., He, D., Li, X., Li, J., and Peng, Z. (2016). Design, Synthesis and Biological Evaluation of Novel Coumarin Thiazole Derivatives as  $\alpha$ -glucosidase Inhibitors. *Bioorg. Chem.* 65, 167–174. doi:10.1016/j.bioorg.2016.03.001
- Wang, G., Wang, J., Xie, Z., Chen, M., Li, L., Peng, Y., et al. (2017). Discovery of 3,3-Di(indolyl)indolin-2-One as a Novel Scaffold for  $\alpha$ -glucosidase Inhibitors: *In Silico* Studies and SAR Predictions. *Bioorg. Chem.* 72, 228–233. doi:10.1016/j.bioorg.2017.05.006
- Wang, Y.-H., Jiang, S.-C., Chen, Y., Guo, T., Xia, R.-J., Tang, X., et al. (2019). Synthesis and Antibacterial Activity of Novel Chalcone Derivatives Bearing a Coumarin Moiety. *Chem. Pap.* 73, 2493–2500. doi:10.1007/s11696-019-00802-0
- Xu, X. T., Deng, X. Y., Chen, J., Liang, Q. M., Zhang, K., Li, D. L., et al. (2019). Synthesis and Biological Evaluation of Coumarin Derivatives as  $\alpha$ -glucosidase Inhibitors. *Eur. J. Med. Chem.* 189, 112013. doi:10.1016/j.ejmech.2019.112013
- Zhong, Y., Yu, L., He, Q., Zhu, Q., Zhang, C., Cui, X., et al. (2019). Bifunctional Hybrid Enzyme-Catalytic Metal Organic Framework Reactors for  $\alpha$ -Glucosidase Inhibitor Screening. *ACS Appl. Mat. Interfaces* 11, 32769–32777. doi:10.1021/acsami.9b11754

**Conflict of Interest:** The authors declare that the research was conducted in the absence of any commercial or financial relationships that could be construed as a potential conflict of interest.

**Publisher's Note:** All claims expressed in this article are solely those of the authors and do not necessarily represent those of their affiliated organizations, or those of the publisher, the editors and the reviewers. Any product that may be evaluated in this article, or claim that may be made by its manufacturer, is not guaranteed or endorsed by the publisher.

Copyright © 2022 Hu, Luo, Wang, Li, Li, Zhang, Xiao, Lu, Xiong, Feng and Li. This is an open-access article distributed under the terms of the Creative Commons Attribution License (CC BY). The use, distribution or reproduction in other forums is permitted, provided the original author(s) and the copyright owner(s) are credited and that the original publication in this journal is cited, in accordance with accepted academic practice. No use, distribution or reproduction is permitted which does not comply with these terms.